Temporal and Noise Behavior of PEAK-GRAPPA

S. Bauer[1], M. Honal[1], B. Jung[1], J. Hennig[1], and M. Markl[1]
[1]Dept. of Diagnostic Radiology, Medical Physics, University Hospital Freiburg, Freiburg, Germany

Introduction: Parallel imaging using the k-space based GRAPPA algorithms has been used for accelerated MR imaging in many applications [1]. Recently, several k-t-space based methods have been introduced to further reduce scan time or to increase resolution of dynamic MR imaging. Techniques such as TGRAPPA[2], k-t GRAPPA[3] or PEAK-GRAPPA [4], k-t-SENSE and k-t BLAST [5] exploit spatial and temporal correlations within time-resolved MR. GRAPPA based methods which directly incorporate temporal correlations into weight estimation are k-t-GRAPPA and PEAK-GRAPPA using a single uniform k-t GRAPPA kernel (fig. 1). It was the aim of this work to provide a detailed analysis of the behavior of PEAK-GRAPPA regarding temporal blurring and SNR performance compared to conventional GRAPPA using a moving and static phantom and in-vivo acquisitions of the heart.

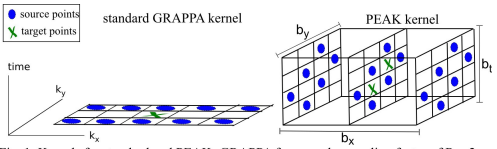

Fig. 1: Kernels for standard and PEAK- GRAPPA for an undersampling factor of R = 2.

Materials and Methods: All measurements were performed on a 3T system (Trio, Siemens, Germany) with full k-space sampling and a 12 channel body coil using an rf-spoiled CINE gradient echo sequence and the following parameters: matrix size = 256x256, temporal resolution = 16.8ms, spatial resolution = 0.94 x 0.94 mm^2. In-vivo imaging was performed with matrix = 214 x 132, temporal resolution = 26ms, spatial resolution = 1.7 x 1.7 mm^2. To obtain the undersampled data, phase encoding lines were subsequently removed and set to zero according to the acceleration factor R and the k-t-GRAPPA sampling scheme (see figure 1, PEAK kernel). Phantom studies were performed using an agarose gel phantom consisting of a moving phantom (see Fig. 2), which oscillated with a frequency of approximately 1 Hz. Additionally a static water bottle was positioned next to the moving phantom.
For SNR estimation an additional acquisition was performed with the same parameters as the phantom measurement but without rf-excitation, i.e. zero flip angle. The autocalibrating lines (N_{acs} = 24) were copied back into k-space after reconstruction. For standard GRAPPA a kernel using b_x x b_y = 5x2 source points was used. For PEAK-GRAPPA a uniform 3D kernel with $b_y = b_t$ = R+d with d=2 for R=2,3 and d = 4 for R>3 and b_x =3 as presented in [4] was used. The lower edge of the moving phantom was selected to analyze image blurring, (fig. 2). A curve fit to a piece-wise defined function was calculated to obtain a quantitative measure of edge sharpness, i.e. blurring (see figure 3). The noise was estimated from the 'noise only' data, which underwent the same reconstruction chain as the measurements with rf-excitation, using the GRAPPA-weights obtained from the acquisition with excitation. To obtain a measure image quality all noise data within the region of the moving phantom were used to generate histograms. The widths of the histograms were used to provide a measure of the noise level for each image.

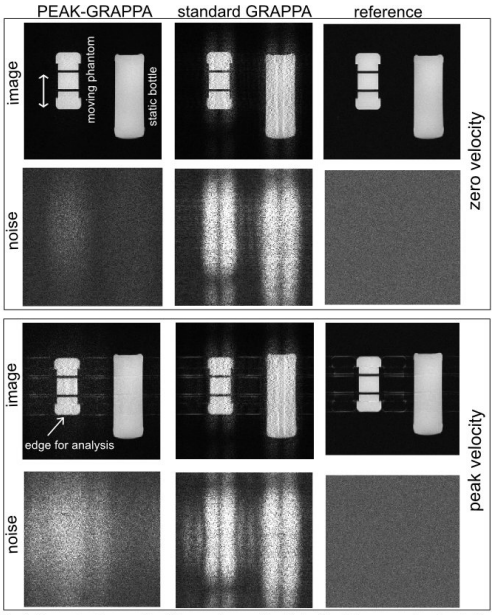

Fig. 2: Reconstruction results with an undersampling factor R = 8 for zero and peak velocity. Additional to each image the reconstruction of the 'noise-only' data is shown.

Results: As an example Fig. 2 shows results for an undersampling factor of R = 8 for two time points during phantom motion at zero (top) and peak velocity (bottom). Note that for 24 ACS lines R = 8 corresponds to a true acceleration of factor of 4.6. Considerable improved SNR performance of PEAK GRAPPA is reflected in the noise images in fig. 2 and the histograms in fig. 3. Compared to standard GRAPPA, PEAK GRAPPA demonstrated markedly reduced spatial noise variation as shown in the histograms in figure 3. Figure 3 also illustrates the noise level (width of histograms) as a function of R for GRAPPA and PEAK-GRAPPA for zero and peak phantom motion. Note that the noise performance of PEAK-GRAPPA exhibited a strong dependence on object motion while, as expected, noise level for standard GRAPPA were independent of object dynamics. Although PEAK GRAPPA showed clearly reduced noise level for zero compared to peak velocity, noise performance was still superior to standard GRAPPA for all R. Fig. 4 shows the mean blurring of the moving phantom edge as a function of the undersampling factor R with only minor blurring for PEAK-GRAPPA. The increase of the blurring for standard GRAPPA is due to the strong noise enhancement for R > 6. The in-vivo results in figure 5 confirm the superior image quality and noise performance of PEAK-GRAPPA at high undersampling factors compared to standard GRAPPA.

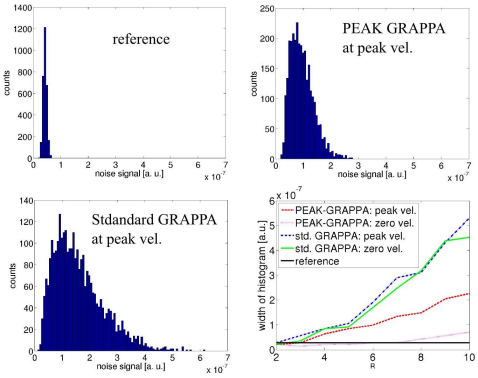

Fig. 3: Histograms of the noise-only images for the moving phantom at peak velocity.The width of the histogram is defined as the width of the distribution at 10 % of the maximum value.

Discussion: Despite the extension of the GRAPPA-Kernel into the time-domain which increases linearly with R, PEAK-GRAPPA shows only minor temporal blurring. Image quality and noise behavior for static objects is considerably improved by PEAK-GRAPPA compared to standard methods. Noise performance SNR of PEAK-GRAPPA is generally superior compared to standard GRAPPA and can provide considerably improved noise performance of more than 100% even at peak velocity. PEAK-GRAPPA may thus provide a very useful tool for dynamic imaging, e.g. cardiovascular MRI. Future work will focus on how variations of the PEAK-GRAPPA kernel geometry may influence the reconstruction results. Another important parameter is the number of ACS lines which should be chosen as small as possible in order to increase the net acceleration factor. The optimal kernel size and the optimal number of ACS lines are closely linked and future studies should thefore focus on the investigation of an optimal combination of kernel geometry, reduction factor and acs lines.

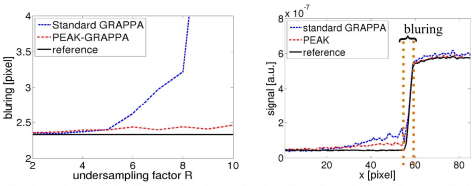

Fig. 4: Bluring analysis of the moving phantom's edge. The left graph shows the mean bluring results dependent on R. The right graph shows the edge for R = 8 and peak velocity.

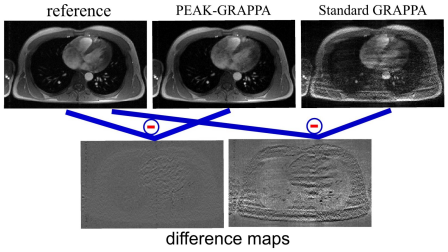

Fig. 5: In vivo results for PEAK-GRAPPA and Standard GRAPPA for a systolic time frame and R = 8, corresponding to an effective acceleration of 3.3. The second row shows the differences to the reference image.

References: [1] Griswold et al. MRM 2002; 47:1202-10 [2] Breuer et al. MRM 2005; 53:981-5 [3] Huang et al. MRM 2005; 54:1172-84 [4] Jung et al. ISMRM 2007:748 [5] Tsao et al. MRM 2003; 50:1031-42
Acknowledgements: Grant support by the Deutsche Forschungsgemeinschaft (DFG), Grant # MA 2383/4-1, and the Bundesministerium für Bildung und Forschung (BMBF), Grant # 01EV0706.